galaxies

Tracked for Impact Factor

CITESCORE 3.3

Article

Applications of the Source-Frequency Phase-Referencing Technique for ngEHT Observations

Wu Jiang, Guang-Yao Zhao, Zhi-Qiang Shen, María J. Rioja, Richard Dodson, Ilje Cho, Shan-Shan Zhao, Marshall Eubanks and Ru-Sen Lu

Special Issue

From Vision to Instrument: Creating a Next-Generation Event Horizon Telescope for a New Era of Black Hole Science

Edited by

Dr. Michael D. Johnson, Dr. Shep Doeleman and Dr. Jose L. Gómez

MDPI

https://doi.org/10.3390/galaxies11010003

galaxies

MDPI

Article

Applications of the Source-Frequency Phase-Referencing Technique for ngEHT Observations

Wu Jiang [1,2,*], Guang-Yao Zhao [3,*], Zhi-Qiang Shen [1,2], María J. Rioja [4,5,6], Richard Dodson [4], Ilje Cho [3], Shan-Shan Zhao [1,2], Marshall Eubanks [7] and Ru-Sen Lu [1,2,8]

1 Shanghai Astronomical Observatory, Chinese Academy of Sciences, Shanghai 200030, China
2 Key Laboratory of Radio Astronomy, Chinese Academy of Sciences, Nanjing 210008, China
3 Instituto de Astrofísica de Andalucía-CSIC, Glorieta de la Astronomía s/n, 18008 Granada, Spain
4 ICRAR, M468, The University of Western Australia, 35 Stirling Hwy, Crawley, WA 6009, Australia
5 CSIRO Astronomy and Space Science, P.O. Box 1130, Bentley, WA 6102, Australia
6 Observatorio Astronómico Nacional (IGN), Alfonso XII, 3 y 5, 28014 Madrid, Spain
7 Space Initiatives Inc., Newport, VA 24128, USA
8 Max-Planck-Institut für Radioastronomie, Auf dem Hügel 69, D-53121 Bonn, Germany
* Correspondence: jiangwu@shao.ac.cn (W.J.); gyzhao@iaa.es (G.-Y.Z.)

Abstract: The source-frequency phase-referencing (SFPR) technique has been demonstrated to have great advantages for mm-VLBI observations. By implementing simultaneous multi-frequency receiving systems on the next-generation Event Horizon Telescope (ngEHT) antennas, it is feasible to carry out a frequency phase transfer (FPT) which could calibrate the non-dispersive propagation errors and significantly increase the phase coherence in the visibility data. Such an increase offers an efficient approach for a weak source or structure detection. The SFPR also makes it possible for high-precision astrometry, including the core-shift measurements up to sub-mm wavelengths for Sgr A*, M 87*, etc. We also briefly discuss the technical and scheduling considerations for future SFPR observations with the ngEHT.

Keywords: black hole; VLBI; ngEHT; astrometry; SFPR

Citation: Jiang, W.; Zhao, G.-Y.; Shen, Z.-Q.; Rioja, M.J.; Dodson, R.; Cho, I.; Zhao, S.-S.; Eubanks, M.; Lu, R.-S. Applications of the Source-Frequency Phase-Referencing Technique for ngEHT Observations. *Galaxies* **2023**, *11*, 3. https://doi.org/10.3390/galaxies11010003

Academic Editor: Luigina Feretti

Received: 15 November 2022
Revised: 10 December 2022
Accepted: 16 December 2022
Published: 21 December 2022

1. Introduction

The Very Long Baseline Interferometry (VLBI) technology can achieve the highest spatial angular resolution by linking intercontinental telescopes to form a virtual telescope, whose aperture size is equal to the longest baseline in the array. However, the wavefront arriving at each telescope suffers from various phase fluctuations when propagating through the atmosphere. This is even more severe at the millimeter and sub-millimeter (sub-mm) wavelengths as the phase dispersion is in proportion to the observing frequency. A novel technique called the frequency phase transfer (FPT) [1] or source-frequency phase referencing (SFPR) [2] is proposed to mitigate the fast phase fluctuations at the shorter wavelengths by referring to the phases at the longer wavelength observed close in time. The phases could be purified by two-step calibrations. The first step is the FPT calibration, where the non-dispersive phase errors, such as the tropospheric phase errors and the geometric antenna position errors, are removed. Furthermore, the unmodeled ionospheric delay and the instrumental phase offsets between the two wavelengths can be further eliminated by observations of a nearby calibrator. After the SFPR calibrations, the remaining phases just reflect the true high-frequency visibilities and the frequency-dependent shift in the positions, e.g., the frequency-dependent location of the jet cores (the core shift) [3]. The SFPR could also help to reliably align the molecular line emission seen at different frequency bands (e.g., [4]). It has great advantages in probing weak sources and high-precision astrometric measuring for the (sub-)mm-VLBI.

The capability of simultaneously receiving at four frequency bands (K/Q/W/D) makes

the Korea VLBI Network (KVN) a unique prototype and instrument for the FPT/SFPR observations [5,6]. The capability of fast switching among receivers at the Very Long Baseline Array (VLBA) also makes it possible to carry out FPT/SFPR observations up to the 3 mm band [2,7], although the switching cycle time introduces coherence losses (see Figure 6 in [8]).

- ngEHT and the necessity of SFPR
  Based on the success of capturing the first images of two nearby supermassive black holes with the original Event Horizon Telescope (EHT), one at the center of the distant Messier 87 galaxy (M87*) [9] and the other at our Milky Way galaxy center (Sgr A*) [10], the next-generation Event Horizon Telescope (ngEHT) will expand the existing array (new sites) [11] and upgrade the technological deployments (receiving capabilities) significantly [12]. It aims to sharpen our view of the black holes and address fundamental questions about the accretion and jet-launching process, together with more black hole shadows captured and even making black hole "movies".
  Although the sensitivity of the ngEHT would be greatly improved with an ultra-wide bandwidth, the baseline sensitivity will still be limited due to the short coherent integration time at sub-mm wavelengths (a typical coherence time is ∼10 s at 230 GHz [13,14] and even shorter at 345 GHz) and the small dish size of most antennas. The SFPR can overcome the coherence time limitation at sub-mm wavelengths. As demonstrated in a separate technical paper in this Special Issue, the coherence time of the high frequency by referring to the low-frequency band could be increased more than 100 folds and extended to hour(s) in the simulations. See Rioja et al. in the same issue for more details. The detection threshold relies on the lower frequency rather than the higher one. Using a typical value of 10–15 s at 85 GHz, the flux density threshold for targets would become one magnitude lower (∼10 mJy) and the number of targets would be hundreds under the array sensitivity. We have estimated the SFPR errors that would be introduced when referencing the 255 or 340 GHz data to 85 GHz, with an angular separation of 10° between sources. With simultaneous multi-frequency observations and intra-source switching times between 0 and 10 min, the astrometric precision is about 3 µas and dominated by the static ionospheric residuals. These would make the ngEHT more powerful for both astrophysical and astrometric applications.

2. Scientific Applications

2.1. Sgr A and M 87**

Sgr A* and M 87* are the prime targets for demonstrating the application of the SFPR to observational studies of black holes and jets. The SFPR can help reduce the phase error budgets from the atmosphere and instruments, while increasing the coherence time, and thus improving the dynamical range of imaging. Furthermore, the SFPR will provide precise measurements to understand the event-horizon-scale structure adjacent to the supermassive black holes.

- Possible core-shift detection of Sgr A*
  The mm/sub-mm radio emission from Sgr A* can be produced by two generic models: an accretion flow itself [15,16] and/or an outflow [17]. To discriminate the dominant emission models of Sgr A* , the core shift, e.g., [3,18], can be used without resolving its structure. As for the jet model, based on GRMHD simulations, Mościbrodzka et al. [19] suggested the core shift of ∼130 µas at 22–43 GHz and ∼60 µas at 86–230 GHz. In a recent study by Fraga-Encinas et al. (in prep.), the core shift of Sgr A* is predicted from both the accretion disk and the jet model with different inclination angles. According to their results, a clear difference in the core shift between the two scenarios is shown. Especially at a small inclination angle, as has been suggested in recent studies [20–22], the expected core shift at 22–43 GHz is $\lesssim$10 µas in the accretion disk model while it is $\gtrsim$100 µas in the jet model. Our preliminary core-shift measurements with the Korean VLBI Network (KVN) and the Very Long Baseline Array (VLBA) at the same frequencies show ∼100 µas (I. Cho et al. in prep). However, the robustness has been

relatively less due to large astrometric uncertainties which are mainly originated from (1) the large beam size (for the KVN) and (2) the frequency switching mode (for the VLBA). Each difficulty can be perfectly overcome through the ngEHT with the dual/triple band receiving capability.

- Connecting the jet and the black hole for M87*
  The EHT 2017 image of M87* has revealed the shadow of the central SMBH [9]. The EHT observations, however, were unable to reliably detect and image the inner jet, likely due to sensitivity limitations and the lack of short baselines in the UV coverage. At longer wavelengths, we see a well-collimated jet, but the emission is optically thick and we are only able to see the $\tau = 1$ surface and the downstream optically thin jet [23]. Furthermore, the resolution at longer wavelengths is not enough to resolve the shadow [24]. It remains uncertain how exactly the SMBH and the jet are connected. The ngEHT will improve the dynamic range of the 1.3 mm images which could enable the detection of the extended jet emission. However, it could be still challenging due to the steep spectrum of the jet. The SFPR covering 86–345 GHz bands offers an alternative way to reliably determine the relative location of the SMBH we see at 1.3 mm and the jet core at longer wavelengths. This is critical in understanding how black holes launch powerful, collimated jets (e.g., [25]).

2.2. *Detection of Weak Sources and Structures*

- Toward more supermassive black hole shadows
  With the increased coherent integration time, black holes, whose radio emissions are weak but shadow sizes are relatively large, can be detected by the ngEHT. According to the prediction of a semi-analytic spectral energy distribution model [26], there should be a dozen additional sources that with their horizon-scale structure resolved the ngEHT observing at 345 GHz [27]. M 84, M 104, and IC 1459 are the prominent candidates on the priority list. These targets have a correlated flux density of several tens mJy [28] and a shadow size of $\sim$10 µas. The sources could be directly fringed with a short solution interval and a relatively high signal-to-noise ratio at 85 GHz that guarantees the quality of the phases to be transferred to higher frequencies. The predicted sizes of the black hole shadows are comparable to the resolution achievable by the ngEHT at 345 GHz. It provides further test samples of black holes, whether or not described by the Kerr metric, besides M87* and Sgr A*. Vice versa, combining the diameter measurements of black hole shadows with GRMHD simulations, plus an independent distance measurement, can be used to determine the physical parameters of black holes (e.g., mass, orientation, spin, etc.).
  Toward understanding black holes, we are still on the road of pursuing precise measurements and conclusive evidence. In the case of M84 (z = 0.00339, D = 18.4 Mpc), the mass of the central supermassive black hole is $8.5 \times 10^8\ M_\odot$ measured by the gas kinematics [29], or $1.8 \times 10^9\ M_\odot$ estimated from the velocity dispersion [30]. Therefore, the diameter d of the black hole shadow would be about 5 or 10 µas, respectively. M 84 has a correlated flux of about 80 mJy at 86 GHz (Wang et al. in press), while the baseline sensitivity of the ngEHT at 86 GHz would achieve several mJy, which would guarantee the phase solutions with a signal-to-noise ratio high enough to be transferred to 345 GHz. As shown in Figure 1, the black hole mass could be independently constrained by the angular size of the shadow. It also indicates that the ngEHT with SFPR could image a batch of black hole shadows whose diameters are $\sim$10 µas. The SFPR could increase the coherent integration time that promises a firm fringe detection at 345 GHz, as well as high dynamic range imaging with a sub-diffraction-limited resolution [31].
- Detection of cosmic sources at 1 mm
  Based on the radio luminosity function, the number of AGNs detectable to the millimeter is almost inversely proportional to the array sensitivity. Besides detecting the horizon structure of faint nearby SMBHs, the SFPR could be used to increase the

detection of cosmic sources at short wavelengths. The flux threshold of the SFPR detection will be ∼10 mJy through simulations. According to the ALMA calibrator catalog (https://almascience.eso.org/sc/, accessed on 1 June 2022), there would be more than nine hundred sources observable. These sources have a correlated flux (considering a resolving factor of ∼0.16 with a baseline length of 5000 km) higher than 10 mJy and a flat spectrum from 85 to 345 GHz. With the increased sensitivity of the ngEHT, which is further enhanced by SFPR, it provides more diverse samples approachable at the upstream of jets for physical parameter statistics, such as the brightness temperature of the mm-core and the collimation profile of the jet base [32,33], as well as sub-structures in the core region [34].

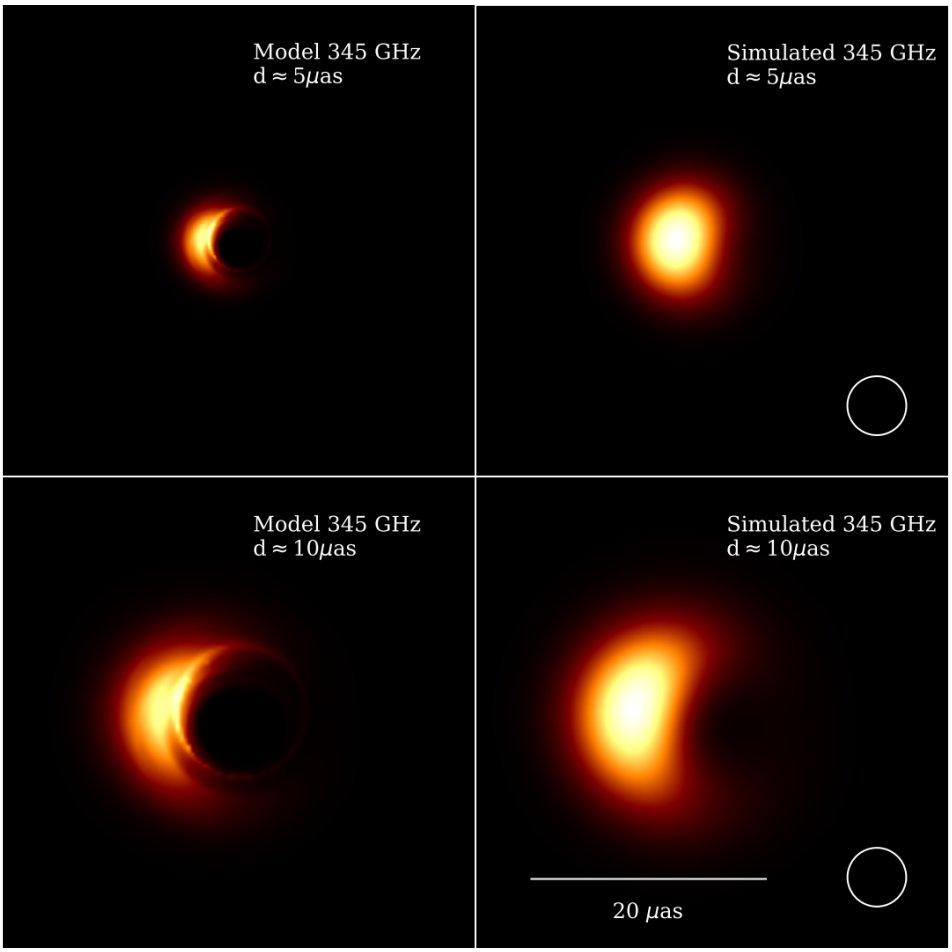

Figure 1. Model images of M84 with two different black hole masses. The images (right column) are reconstructed based on simulated ngEHT observations at 345 GHz. The empty white ring at the right bottom corner of the right panel plots is the synthesized beam of ngEHT at 345 GHz.

2.3. Microarcsecond Astrometry to the Black Holes

SFPR enables the VLBI astrometry at millimeter/sub-millimeter wavelengths with a precision of several μas. That means 0.01 pc motions of targets can be measured within a distance of Gpc. By source-frequency phase referencing, the location of a black hole could be pinpointed [28]. It enables the microarcsecond astrometry to the black hole itself in the ngEHT era.

- Orbit tracking of supermassive black hole binaries
  The merger of galaxies with central black holes can lead to the formation of a compact supermassive black hole binary (SMBHB) at the new galaxy center [35]. The early dynamical friction-driven and late gravitational radiation-driven phases of the SMBHB evolution are separated by the sub-pc orbital separation regime. How does the SMBHB

overcome this regime is known as the final-parsec problem [36]. For the ngEHT with SFPR, the propagation delays caused by the troposphere could be canceled out; we can still rely on a signal-to-noise-ratio-dependent resolution. The astrometric tracking of a black hole from an SMBHB system can reach 1 μas precision or better [37,38]. In the calculation of a population of detectable SMBHBs, we adopt the fiducial parameters of the model with a larger maximum observed binary period $P_{base} = 30$ yr (see Table 1 in [38]) and plot the number of SMBHBs as a function of the resolution θ_{min} and the sensitivity F_{min} (Figure 2). The ngEHT would provide an opportunity to track several observable sub-pc SMBHBs with a threshold of $\theta_{min} = 15$ μas and $F_{min} = 10$ mJy. While considering tracking the orbit motions of an SMBHB with respect to a background source in the same field as the upper limit, the minimum threshold of θ_{min} and F_{min} is 1 μas (the static ionospheric residuals could be minimized in the in-beam scenario) and 1 mJy, respectively, as shown in Figure 2.

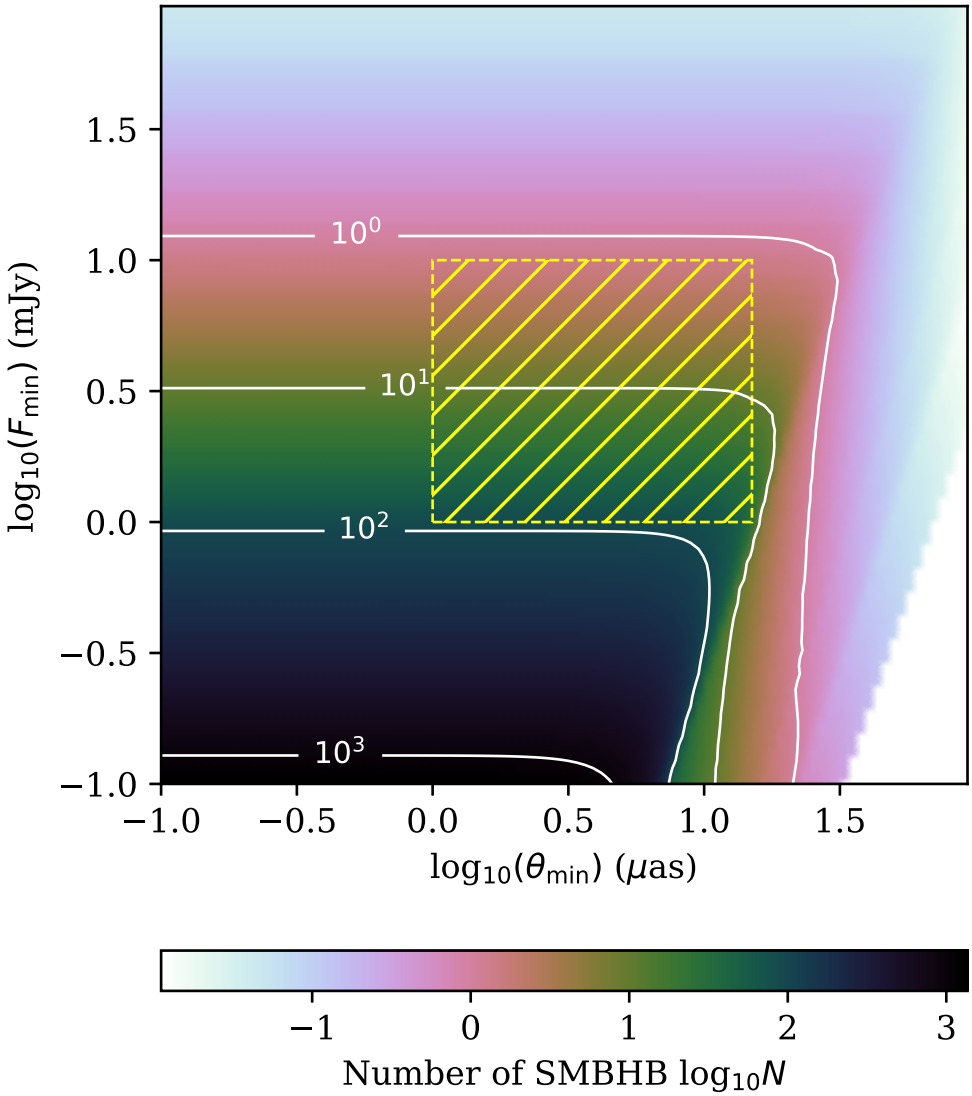

Figure 2. Number of detectable SMBHB systems (redshift z < 0.5) for the orbital tracking as a function of two main array parameters: the resolution θ_{min} and the sensitivity F_{min}. The hatched area is the target region by ngEHT, where it uses the baseline sensitivity of 10 mJy and the resolution of 15 microarcsec as the lower limit of the detection number of supermassive black hole binary systems, while the upper limit of the number is roughly corresponding to the array sensitivity and the precision of proper motion measurement by ngEHT, considering a background calibrator in the same field.

- Relative and absolute astrometric measurements
  The direct astrometric output of the SFPR is the core shift. It can be the relative positions between the 85 GHz core and the photon ring of the black hole when the 340 GHz already reaches the horizon scale. Otherwise, the core shift can be used to estimate the magnetic field and the particle density of the innermost jet [39], as well as predicting the jet apex up to the infinite frequency [3]. This provides a capability to position the black hole and track its motions by synergy with the lower-frequency VLBI, where the absolute astrometry is possible. Meanwhile, the absolute astrometry at short wavelengths needs cluster/paired antennas in each site [37]. The current proper motions of SgrA* still suffer from the scattering as measured at 43 GHz [40,41]; if one can go to a higher frequency, this effect can be largely reduced at the ngEHT frequencies. This is also very important to understand the head–tail sources (e.g., IC 310 and NGC 1265) whose hosting galaxies are infalling into the cluster at a high speed [42].

3. Requirements

3.1. Instrumentation Requirement

The capability of simultaneous observations at a lower-frequency band (85 or 110 GHz, 3 mm) and at one or two higher-frequency bands (255 or 220 GHz, 1.2 mm, and 340 or 330 GHz, 0.88 mm) is required for the frequency phase transfer. This can be accomplished with a quasi-optics tri-band receiving system [43] or a wide-band receiver [44]. In the case of a large interferometry array or co-site antennas working as a single VLBI station, the capability of forming sub-arrays corresponding to the lower and the higher observing frequency bands is feasible compared to installing trip-band receivers for each antenna. A co-located GPS will give accurate site positions for the geometric model, and the root mean square of the tropospheric path length fluctuations should be monitored for the co-site antennae. These have been found to greatly reduce the residual ionospheric, positional, and tropospheric contributions. Fuller descriptions of their impact can be found in [45]. The planned recording data rate as high as 256 Gbps would be able to incorporate the multi-band data stream simultaneously because the available bandwidth will be shared across all bands. The baseline sensitivity should be high enough to guarantee the fringe detection and minimize the phase errors on a correlated flux of a $\sim$10 mJy source at the lower frequency, as well as to achieve a super/over-resolution power [31,46]. A detailed technical demand on the instruments is presented by Rioja et al. in the same Special Issue.

3.2. Strategy of Observation and Calibration

SFPR allows a phase calibrator within 10° apart in the sky and a switching cycle of more than 10 min [2]. SFPR expects a calibrator of a correlated flux higher enough at both the low- and high-frequency bands that could be fringed. A higher flux is better so as to mainly reduce the thermal noise. Meanwhile, a relatively large separation, i.e., 10°, makes it much less restrictive to find a suitable calibrator even at the high frequencies. The core shift of the phase calibrator would be incorporated into the final core-shift measurement [6,47]. A prior core shift of a calibrator or a negligible core shift at the RA or DEC direction would be helpful to extract the true core shift of the target [7,28]. A synergy with the lower-frequency VLBI networks observing simultaneously can obtain more core-shift measurements to fit the power law scheme and perform the absolute astrometry observations.

4. Summary

With the aid of a simultaneous multi-frequency receiving system and more new stations available [6,8], the ngEHT with SFPR technique will be a very powerful tool to investigate the accretion disk and the jet/outflow connection in Sgr A* and M 87*, or other interesting targets at sub-mm wavelengths. With a dramatically increased coherence time and more feasible observational requirements (e.g., a long switching cycle time and large

angular separation of calibrators), it will help to capture more images of black hole shadows and detect black hole motions in a binary system or a galaxy cluster.

Author Contributions: Conceptualization, W.J., G.-Y.Z. and Z.-Q.S.; methodology, W.J., G.-Y.Z., M.-J.R. and R.D.; software, S.-S.Z. and W.J.; writing—original draft preparation, W.J., G.-Y.Z. and I.C.; writing—review and editing, W.J., G.-Y.Z., Z.-Q.S., M.J.R., R.D., I.C., R.-S.L. and M.E. All authors have read and agreed to the published version of the manuscript.

Funding: This work was supported in part by the National Natural Science Foundation of China (grant Nos. 12173074, 11803071, and 11933007), the Key Research Program of Frontier Sciences, CAS (grant Nos. QYZDJ-SSW-SLH057 and ZDBS-LY-SLH011), the Shanghai Pilot Program for Basic Research—Chinese Academy of Science, Shanghai Branch (JCYJ-SHFY-2022-013), the Spanish Ministerio de Economía y Competitividad (grants AYA2016-80889-P and PID2019-108995GB-C21), the Consejería de Economía, Conocimiento, Empresas y Universidad of the Junta de Andalucía (grant P18-FR-1769), the Consejo Superior de Investigaciones Científicas (grant 2019AEP112), and the State Agency for Research of the Spanish MCIU through the "Center of Excellence Severo Ochoa" award to the Instituto de Astrofísica de Andalucía (SEV-2017-0709).

Institutional Review Board Statement: Not applicable.

Informed Consent Statement: Not applicable.

Data Availability Statement: Not applicable.

Acknowledgments: We thank the referees for their constructive comments and suggestions.

Conflicts of Interest: The authors declare no conflict of interest.

References

1. Middelberg, E.; Roy, A.L.; Walker, R.C.; Falcke, H. VLBI observations of weak sources using fast frequency switching. *A&A* **2005**, *433*, 897–909. [CrossRef]
2. Rioja, M.; Dodson, R. High-precision Astrometric Millimeter Very Long Baseline Interferometry Using a New Method for Atmospheric Calibration. *AJ* **2011**, *141*, 114. [CrossRef]
3. Lobanov, A.P. Ultracompact jets in active galactic nuclei. *A&A* **1998**, *330*, 79–89.
4. Yoon, D.H.; Cho, S.H.; Yun, Y.; Choi, Y.K.; Dodson, R.; Rioja, M.; Kim, J.; Imai, H.; Kim, D.; Yang, H.; et al. Astrometrically registered maps of H_2O and SiO masers toward VX Sagittarii. *Nat. Commun.* **2018**, *9*, 2534. [CrossRef]
5. Rioja, M.J.; Dodson, R.; Jung, T.; Sohn, B.W. The Power of Simultaneous Multifrequency Observations for mm-VLBI: Astrometry up to 130 GHz with the KVN. *AJ* **2015**, *150*, 202. [CrossRef]
6. Zhao, G.Y.; Jung, T.; Sohn, B.W.; Kino, M.; Honma, M.; Dodson, R.; Rioja, M.; Han, S.T.; Shibata, K.; Byun, D.Y.; et al. Source-Frequency Phase-Referencing Observation of AGNS with KAVA Using Simultaneous Dual-Frequency Receiving. *J. Korean Astron. Soc.* **2019**, *52*, 23–30. [CrossRef]
7. Jiang, W.; Shen, Z.; Jiang, D.; Martí-Vidal, I.; Kawaguchi, N. VLBI Imaging of M81* at λ = 3.4 mm with Source-frequency Phase-referencing. *ApJL* **2018**, *853*, L14. [CrossRef]
8. Rioja, M.J.; Dodson, R. Precise radio astrometry and new developments for the next-generation of instruments. *AApR* **2020**, *28*, 6. [CrossRef]
9. Event Horizon Telescope Collaboration; Akiyama, K.; Alberdi, A.; Alef, W.; Asada, K.; Azulay, R.; Baczko, A.K.; Ball, D.; Baloković, M.; Barrett, J.; et al. First M87 Event Horizon Telescope Results. I. The Shadow of the Supermassive Black Hole. *Astrophys. J. Lett.* **2019**, *875*, L1. [CrossRef]
10. Event Horizon Telescope Collaboration; Akiyama, K.; Alberdi, A.; Alef, W.; Algaba, J.C.; Anantua, R.; Asada, K.; Azulay, R.; Bach, U.; Baczko, A.K.; et al. First Sagittarius A* Event Horizon Telescope Results. I. The Shadow of the Supermassive Black Hole in the Center of the Milky Way. *ApJL* **2022**, *930*, L12. [CrossRef]
11. Raymond, A.W.; Palumbo, D.; Paine, S.N.; Blackburn, L.; Córdova Rosado, R.; Doeleman, S.S.; Farah, J.R.; Johnson, M.D.; Roelofs, F.; Tilanus, R.P.J.; et al. Evaluation of New Submillimeter VLBI Sites for the Event Horizon Telescope. *ApJS* **2021**, *253*, 5. [CrossRef]
12. Doeleman, S.; Blackburn, L.; Doeleman, S.; Dexter, J.; Gomez, J.L.; Johnson, M.D.; Palumbo, D.C.; Weintroub, J.; Farah, J.R.; Fish, V.; et al. Studying Black Holes on Horizon Scales with VLBI Ground Arrays. In Proceedings of the Bulletin of the American Astronomical Society, 2019; Volume 51, p. 256.
13. Blackburn, L.; Chan, C.k.; Crew, G.B.; Fish, V.L.; Issaoun, S.; Johnson, M.D.; Wielgus, M.; Akiyama, K.; Barrett, J.; Bouman, K.L.; et al. EHT-HOPS Pipeline for Millimeter VLBI Data Reduction. *ApJ* **2019**, *882*, 23. [CrossRef]
14. Event Horizon Telescope Collaboration; Akiyama, K.; Alberdi, A.; Alef, W.; Asada, K.; Azulay, R.; Baczko, A.K.; Ball, D.; Baloković, M.; Barrett, J.; et al. First M87 Event Horizon Telescope Results. III. Data Processing and Calibration. *ApJL* **2019**, *875*, L3. [CrossRef]

15. Narayan, R.; Yi, I.; Mahadevan, R. Explaining the spectrum of Sagittarius A* with a model of an accreting black hole. *Nature* **1995**, *374*, 623–625. [CrossRef]
16. Yuan, F.; Quataert, E.; Narayan, R. Nonthermal Electrons in Radiatively Inefficient Accretion Flow Models of Sagittarius A*. *ApJ* **2003**, *598*, 301–312. [CrossRef]
17. Falcke, H.; Markoff, S. The jet model for Sgr A*: Radio and X-ray spectrum. *A&A* **2000**, *362*, 113–118.
18. Blandford, R.D.; Königl, A. Relativistic jets as compact radio sources. *ApJ* **1979**, *232*, 34–48. [CrossRef]
19. Mościbrodzka, M.; Falcke, H.; Shiokawa, H.; Gammie, C.F. Observational appearance of inefficient accretion flows and jets in 3D GRMHD simulations: Application to Sagittarius A*. *A&A* **2014**, *570*, A7. [CrossRef]
20. Gravity Collaboration; Abuter, R.; Amorim, A.; Bauböck, M.; Berger, J.P.; Bonnet, H.; Brand ner, W.; Clénet, Y.; Coudé Du Foresto, V.; de Zeeuw, P.T.; et al. Detection of orbital motions near the last stable circular orbit of the massive black hole SgrA*. *A&A* **2018**, *618*, L10. [CrossRef]
21. Issaoun, S.; Johnson, M.D.; Blackburn, L.; Brinkerink, C.D.; Mościbrodzka, M.; Chael, A.; Goddi, C.; Martí-Vidal, I.; Wagner, J.; Doeleman, S.S.; et al. The Size, Shape, and Scattering of Sagittarius A* at 86 GHz: First VLBI with ALMA. *ApJ* **2019**, *871*, 30. [CrossRef]
22. Cho, I.; Zhao, G.Y.; Kawashima, T.; Kino, M.; Akiyama, K.; Johnson, M.D.; Issaoun, S.; Moriyama, K.; Cheng, X.; Algaba, J.C.; et al. The Intrinsic Structure of Sagittarius A* at 1.3 cm and 7 mm. *ApJ* **2022**, *926*, 108. [CrossRef]
23. Hada, K.; Doi, A.; Kino, M.; Nagai, H.; Hagiwara, Y.; Kawaguchi, N. An origin of the radio jet in M87 at the location of the central black hole. *Nature* **2011**, *477*, 185–187. [CrossRef]
24. EHT MWL Science Working Group; Algaba, J.C.; Anczarski, J.; Asada, K.; Baloković, M.; Chandra, S.; Cui, Y.Z.; Falcone, A.D.; Giroletti, M.; Goddi, C.; et al. Broadband Multi-wavelength Properties of M87 during the 2017 Event Horizon Telescope Campaign. *ApJL* **2021**, *911*, L11. [CrossRef]
25. Blandford, R.; Meier, D.; Readhead, A. Relativistic Jets from Active Galactic Nuclei. *Annu. Rev. Astron. Astrophys.* **2019**, *57*, 467–509. [CrossRef]
26. Huang, L.; Takahashi, R.; Shen, Z.Q. Testing the Accretion Flow with Plasma Wave Heating Mechanism for Sagittarius A* by the 1.3 mm VLBI Measurements. *ApJ* **2009**, *706*, 960–969. [CrossRef]
27. Pesce, D.W.; Palumbo, D.C.M.; Narayan, R.; Blackburn, L.; Doeleman, S.S.; Johnson, M.D.; Ma, C.P.; Nagar, N.M.; Natarajan, P.; Ricarte, A. Toward Determining the Number of Observable Supermassive Black Hole Shadows. *ApJ* **2021**, *923*, 260. [CrossRef]
28. Jiang, W.; Shen, Z.; Martí-Vidal, I.; Wang, X.; Jiang, D.; Kawaguchi, N. Millimeter-VLBI Observations of Low-luminosity Active Galactic Nuclei with Source-frequency Phase Referencing. *ApJL* **2021**, *922*, L16. [CrossRef]
29. Walsh, J.L.; Barth, A.J.; Sarzi, M. The Supermassive Black Hole in M84 Revisited. *ApJ* **2010**, *721*, 762–776. [CrossRef]
30. Ly, C.; Walker, R.C.; Wrobel, J.M. An Attempt to Probe the Radio Jet Collimation Regions in NGC 4278, NGC 4374 (M84), and NGC 6166. *AJ* **2004**, *127*, 119–124. [CrossRef]
31. Akiyama, K.; Kuramochi, K.; Ikeda, S.; Fish, V.L.; Tazaki, F.; Honma, M.; Doeleman, S.S.; Broderick, A.E.; Dexter, J.; Mościbrodzka, M.; et al. Imaging the Schwarzschild-radius-scale Structure of M87 with the Event Horizon Telescope Using Sparse Modeling. *ApJ* **2017**, *838*, 1. [CrossRef]
32. Asada, K.; Nakamura, M.; Pu, H.Y. Indication of the Black Hole Powered Jet in M87 by VSOP Observations. *ApJ* **2016**, *833*, 56. [CrossRef]
33. Janssen, M.; Falcke, H.; Kadler, M.; Ros, E.; Wielgus, M.; Akiyama, K.; Baloković, M.; Blackburn, L.; Bouman, K.L.; Chael, A.; et al. Event Horizon Telescope observations of the jet launching and collimation in Centaurus A. *Nat. Astron.* **2021**, *5*, 1017–1028. [CrossRef]
34. Giovannini, G.; Savolainen, T.; Orienti, M.; Nakamura, M.; Nagai, H.; Kino, M.; Giroletti, M.; Hada, K.; Bruni, G.; Kovalev, Y.Y.; et al. A wide and collimated radio jet in 3C84 on the scale of a few hundred gravitational radii. *Nat. Astron.* **2018**, *2*, 472–477. [CrossRef]
35. Kormendy, J.; Ho, L.C. Coevolution (Or Not) of Supermassive Black Holes and Host Galaxies. *ARAA* **2013**, *51*, 511–653. [CrossRef]
36. Begelman, M.C.; Blandford, R.D.; Rees, M.J. Massive black hole binaries in active galactic nuclei. *Nature* **1980**, *287*, 307–309. [CrossRef]
37. Broderick, A.E.; Loeb, A.; Reid, M.J. Localizing Sagittarius A* and M87 on Microarcsecond Scales with Millimeter Very Long Baseline Interferometry. *ApJ* **2011**, *735*, 57. [CrossRef]
38. D'Orazio, D.J.; Loeb, A. Repeated Imaging of Massive Black Hole Binary Orbits with Millimeter Interferometry: Measuring Black Hole Masses and the Hubble Constant. *ApJ* **2018**, *863*, 185. [CrossRef]
39. Zamaninasab, M.; Clausen-Brown, E.; Savolainen, T.; Tchekhovskoy, A. Dynamically important magnetic fields near accreting supermassive black holes. *Nature* **2014**, *510*, 126–128. [CrossRef]
40. Reid, M.J.; Brunthaler, A. The Proper Motion of Sagittarius A*. II. The Mass of Sagittarius A*. *ApJ* **2004**, *616*, 872–884. [CrossRef]
41. Xu, S.J.; Zhang, B.; Reid, M.J.; Zheng, X.W.; Wang, G.L.; Jung, T. A Milliarcsecond Accurate Position for Sagittarius A*. *ApJ* **2022**. [CrossRef]
42. Gendron-Marsolais, M.; Hlavacek-Larrondo, J.; van Weeren, R.J.; Rudnick, L.; Clarke, T.E.; Sebastian, B.; Mroczkowski, T.; Fabian, A.C.; Blundell, K.M.; Sheldahl, E.; et al. High-resolution VLA low radio frequency observations of the Perseus cluster: Radio lobes, mini-halo, and bent-jet radio galaxies. *Mon. Not. R. Astron. Soc.* **2020**, *499*, 5791–5805. [CrossRef]

43. Han, S.T.; Lee, J.W.; Kang, J.; Oh, C.S.; Byun, D.Y.; Je, D.H.; Chung, M.H.; Wi, S.O.; Song, M.; Kang, Y.W.; et al. Korean VLBI Network Receiver Optics for Simultaneous Multifrequency Observation: Evaluation. *Publ. Astron. Soc. Pac.* **2013**, *125*, 539. [CrossRef]
44. Yamasaki, Y.; Masui, S.; Ogawa, H.; Kondo, H.; Matsumoto, T.; Okawa, M.; Yokoyama, K.; Minami, T.; Konishi, R.; Kawashita, S.; et al. Development of a new wideband heterodyne receiver system for the Osaka 1.85 m mm-submm telescope: Corrugated horn and optics covering the 210-375 GHz band. *PASJ* **2021**, *73*, 1116–1127. [CrossRef]
45. Thompson, A.R.; Moran, J.M.; Swenson, G.W.J. *Interferometry and Synthesis in Radio Astronomy*, 2nd ed.; Springer International Publishing: Cham, Switzerland, 2001.
46. Martí-Vidal, I.; Pérez-Torres, M.A.; Lobanov, A.P. Over-resolution of compact sources in interferometric observations. *A&A* **2012**, *541*, A135. [CrossRef]
47. Jung, T.; Dodson, R.; Han, S.T.; Rioja, M.J.; Byun, D.Y.; Honma, M.; Stevens, J.; de Vincente, P.; Sohn, B.W. Measuring the Core Shift Effect in AGN Jets with the Extended Korean VLBI Network. *J. Korean Astron. Soc.* **2015**, *48*, 277–284. [CrossRef]